Ab initio potential energy curves of the valence, Rydberg, and ion-pair states of iodine monochloride, ICl

Apostolos Kalemos and Rita Prosmiti

Articles you may be interested in

Ab initio study of valence and Rydberg states of CH 3 Br
J. Chem. Phys. **130**, 244306 (2009); 10.1063/1.3152865

On the R -dependence of the spin-orbit coupling constant: Potential energy functions of Xe 2 + by high-resolution photoelectron spectroscopy and ab initio quantum chemistry
J. Chem. Phys. **128**, 234306 (2008); 10.1063/1.2937133

Extensive ab initio study of the valence and low-lying Rydberg states of BBr including spin-orbit coupling
J. Chem. Phys. **124**, 194307 (2006); 10.1063/1.2197830

Global ab initio potential energy surfaces for the lowest three doublet states (1 2 A ′ , 2 2 A ′ , and 1 2 A ″) of the BrH 2 system
J. Chem. Phys. **119**, 7838 (2003); 10.1063/1.1609398

Ab initio relativistic all-electron calculation of the Ar–I 2 ground state potential
J. Chem. Phys. **109**, 359 (1998); 10.1063/1.476572

Ab initio potential energy curves of the valence, Rydberg, and ion-pair states of iodine monochloride, ICl

Apostolos Kalemos[1,a)] and Rita Prosmiti[2]

[1]*Laboratory of Physical Chemistry, Department of Chemistry, National and Kapodistrian University of Athens, Athens 15771, Greece*

[2]*Instituto de Física Fundamental, Consejo Superior de Investigaciones Científicas, (IFF-CSIC), Serrano 123, 28006 Madrid, Spain*

We present for the first time a coherent *ab initio* study of 39 states of valence, Rydberg, and ion-pair character of the diatomic interhalogen ICl species through large scale multireference variational methods including spin-orbit effects coupled with quantitative basis sets. Various avoided crossings are responsible for a non-adiabatic behaviour creating a wonderful vista for its theoretical description. Our molecular constants are compared with all available experimental data with the aim to assist experimentalists especially in the high energy regime of up to ∼95 000 cm^{-1}. © *2014 AIP Publishing LLC*. [http://dx.doi.org/10.1063/1.4894771]

I. INTRODUCTION

The first experimental investigation of iodine monochloride was the discovery of a number of faint bands just beyond the convergence of the v″ = 0 progression around 5755 Å by Gibson and Ramsperger[1] and by Gibson and Rice[2] in the late 1920s. Since then numerous experiments have been performed probing several valence,[3–24] ion-pair,[11,17,25–35] and Rydberg[31,36,37] states via numerous techniques such as visible absorption spectroscopy, emission spectroscopy, laser-induced fluorescence spectroscopy, vacuum ultraviolet spectroscopy, and micro- and millimeter-wave spectroscopy.
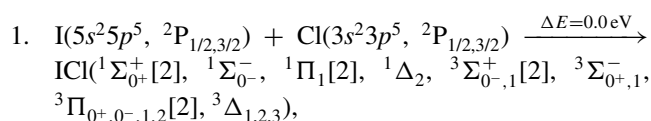
Despite the wealth of experimental data accumulated over all these years the theoretical studies are limited to only a handful of papers. The very first theoretical investigation appeared by Balasubramanian[39] who in 1985 constructed potential energy curves (PEC) for several low lying valence Ω states employing relativistic effective potentials for the I atom and a double ζ Slater basis set for the $4d^{10}5s^25p^5$/$_I$ and all Cl electrons. With an eye to the interpretation of photodissociation processes in the first and second absorption bands at 270 and 470 nm, respectively (e.g., see Refs. 40 and 41 and references therein), Yabushita and co-workers[42] calculated PECs of Ω states dissociating to two ns^2np^5 $^2P_{1/2,3/2}$ state atoms and discussed the avoided crossings and first order non-adiabatic effects. The effect of the long range potential interactions on the polarization of the Cl atoms from the UV photodissociation of ICl has also been investigated[43] combining spectroscopic, *ab initio* and perturbation theory data. The above two sets of theoretical investigations are supplemented by the study of few ion-pair states[44] and by some earlier publications whose main objective is the combined study of relativistic and correlation effects on the properties of heavy diatomic interhalogens.[45]

It is clear that there is an imbalance in what we know about this molecule from an experimental and from a theoretical point of view. With the aim to improve this situation, and at the same time to trigger future work just like the recent velocity map imaging experiments on the photodissociation mechanism of high-lying Rydberg states of molecular iodine via ion-pair states,[46] we report a detailed investigation of several Ω states dissociating adiabatically not only to two valence state atoms, i.e., I or Cl in ns^2np^5, $^2P_{1/2,3/2}$ but also to Rydberg states whose PECs display numerous avoided crossings due to ion-pair states, to electrostatic and spin-orbit (SO) effects, creating that way a "marvelous" non-adiabatic *milieu* for the nuclear motion.

From a computational point of view, diatomic (inter) halogens XX′ (X, X′ = F, Cl, Br, and I) are species of intricate difficulties due to the rather large number of valence (7 + 7 = 14 e^-) and core (or subvalence) electrons (18(I) + 8(Cl) = 26 e^-) as well as to the Rydberg character of their excited states intermingled with charge-transfer (or ion-pair) states.[47] Apart from the pure academic interest for their *per se* study additional interest is found in collisional processes with rare gas atoms forming van der Waals complexes[48,49] and in solvation effects in He and Xe clusters.[50,51] In an effort to shed some light on the electronic structure of ICl, that is relatively speaking poorly known, we have constructed multireference MRCI+SO PECs for several ICl states employing large basis sets.

II. COMPUTATIONAL METHODS

For the ICl diatomic species the first few adiabatic dissociation channels based on a term-order classification scheme according to the Moore/NIST[52] tables along with the resulting $^{2S+1}\Lambda_\Omega$ molecular states are

1. I($5s^25p^5$, $^2P_{1/2,3/2}$) + Cl($3s^23p^5$, $^2P_{1/2,3/2}$) $\xrightarrow{\Delta E=0.0\,\text{eV}}$ ICl($^1\Sigma_{0^+}^+[2]$, $^1\Sigma_{0^-}^-$, $^1\Pi_1[2]$, $^1\Delta_2$, $^3\Sigma_{0^-,1}^+[2]$, $^3\Sigma_{0^+,1}^-$, $^3\Pi_{0^+,0^-,1,2}[2]$, $^3\Delta_{1,2,3}$),

a)kalemos@chem.uoa.gr

141, 104312-1

2. $I(5s^25p^4(^3P)6s^1, \ ^4P_{5/2,3/2,1/2}) \ + \ Cl(3s^23p^5, \ ^2P_{1/2,3/2})$
    $\xrightarrow{\Delta E=6.886 \, eV} \ ICl(^3\Sigma^+_{0^-,1}, \ ^3\Sigma^-_{0^+,1}[2], \ ^3\Pi_{0^+,0^-,1,2}[2],$
    $^3\Delta_{1,2,3}, \quad ^5\Sigma^+_{0^-,1,2}, \quad ^5\Sigma^-_{0^+,1,2}[2], \quad ^5\Pi_{0^+,0^-,1,-1,2,3}[2],$
    $^5\Delta_{0^+,0^-,1,2,3,4}),$

3. $I(5s^25p^4(^3P)6s^1, \ ^2P_{3/2,1/2}) \ + \ Cl(3s^23p^5, \ ^2P_{1/2,3/2})$
    $\xrightarrow{\Delta E=6.934 \, eV} \ ICl(^1\Sigma^+_{0^+}, \ ^1\Sigma^-_{0^-}[2], \ ^1\Pi_1[2], \ ^1\Delta_2, \ ^3\Sigma^+_{0^-},$
    $^3\Sigma^-_{0^+,1}[2], \ ^3\Pi_{0^+,0^-,1,2}[2], \ ^3\Delta_{1,2,3}),$

4. $I(5s^25p^4(^3P)6p^1, \ ^4P) \ + \ Cl(3s^23p^5, \ ^2P) \ \xrightarrow{\Delta E=7.744 \, eV}$
    $ICl(^3\Sigma^+_{0^-,1}, \quad ^3\Sigma^-_{0^+,1}[2], \quad ^3\Pi_{0^+,0^-,1,2}[2], ^3\Delta_{1,2,3}, ^5\Sigma^+_{0^-,1,2},$
    $^5\Sigma^-_{0^+,1,2}[2], ^5\Pi_{0^+,0^-,1,-1,2,3}[2], ^5\Delta_{0^+,0^-,1,2,3,4}),$

5. $I(5s^25p^4(^1D)6s^1, \ ^2D) \ + \ Cl(3s^23p^5, \ ^2P) \ \xrightarrow{\Delta E=8.202 \, eV}$
    $ICl(^1\Sigma^+_{0^+}[2], \qquad\qquad ^1\Sigma^-_{0^-}, ^1\Pi_1[3], ^1\Delta_2[2], ^1\Phi_3, ^3\Sigma^+_{0^-,1}[2],$
    $^3\Sigma^-_{0^+,1}, \ ^3\Pi_{0^+,0^-,1,2}[3], ^3\Delta_{1,2,3}[2], ^3\Phi_{2,3,4}).$

Two more dissociation channels of ion-pair character are relevant to the present study, the $I^+(5s^25p^4, \ ^3P$ and $^1D)$ $+ \ Cl^-(3s^23p^6, \ ^1S)$ at $\Delta E = 6.83$ and 8.15 eV above the ground state fragments,[52] respectively. The number of Ω states resulting from this limited set of adiabatic channels is extremely large and practically impossible to calculate in its totality by any computational method available today. It is also clear that the complexity would be enormous while any post Born–Oppenheimer (BO) treatment for the nuclear motion problem should be well focused on the experimental problem to be solved since a general "all states of the same symmetry treatment" may be simply intractable.

We have constructed valence $(14 \ e^-)$ internally contracted MRCI[53(a)]+SO PECs for 39 molecular states using the relativistic ECP28MDF effective core potential for the [Ar $+ \ 3d^{10}$] electrons of I while for its $4s^24p^64d^{10}5s^25p^5$ electrons the aug-cc-pV5Z-PP $(17s14p14d4f3g2h)$ basis set[54(a)] is used generally contracted to $[8s8p6d4f3g2h]$. For the Cl atom the all electron aug-cc-pV(5+d)Z basis set[54(b)] $(21s13p6d4f3g2h)$ generally contracted to $[8s7p6d4f3g2h]$ has been employed. Core–valence (CV) correlation effects have been accounted for by both the MRCI(+Q) and the restricted coupled cluster + single + double + perturbative connected triplets (RCCSD(T))[53(b)] computational methods coupled with the appropriately optimized CV basis sets, i.e., the cc-pwCV5Z-PP[54(c)] $(20s17p17d7f5g3h1i)$ $\rightarrow [11s11p9d7f5g3h1i]$ for the I $4s^24p^64d^{10}5s^25p^5$ electrons and the cc-pwCV5Z $(20s12p8d6f4g2h)\rightarrow[11s10p8d6f4g2h]$ for Cl.[54(d)] Thus the ICl diatomic $(70–28 = 42 \ e^-$ system) is described by the valence $[8s8p6d4f3g2h/_I \ 8s7p6d4f3g2h/_{Cl}]$ and CV $[11s11p9d7f5g3h1i/_I \ 11s10p8d6f4g2h/_{Cl}]$ basis sets consisting of 275 and 410 spherical Gaussian functions, respectively. The one electron basis set (molecular orbitals) was generated through the complete active space SCF (CASSCF)[53(c)] zeroth order wavefunction with active spaces ranging from the usual valence space $(5p(I) + 3p(Cl))$ for all states correlating to two ground ^2P atomic states, augmented by either a Rydberg s orbital for all $^1\Lambda$ states correlating to the ^4P or ^2P Rydberg atomic I states or one s and three Rydberg $p_{(x,y,z)}$ orbitals for all $^3\Lambda$ states dissociating to the corresponding atomic Rydberg states of the I atom. The $3s^2(Cl)$ and $5s^2(I)$ electrons are not distributed in the above mentioned active spaces of the CASSCF wavefunction since the practically

full np shell cannot provide any angular type dynamic correlation for the ns^2 electrons which are nevertheless fully correlated in all subsequent MRCI and RCCSD(T) calculations. These correlation effects have been assessed by distributing all 14 valence electrons in the space of $8 + 5 = 13$ orbitals, the additional 5 orbitals of primarily d(Cl) character were determined at the CI level for states of $^1A_1$ symmetry (*vide infra*). The MRCI wavefunctions form the basis for the SO (LS operator in the MOLPRO code)[53(d)] calculations that take into account the ECP spin-orbit operator for the I atom and the full Breit Pauli operator for the Cl atom.

The molecular parameters, i.e., dissociation energies D_e, harmonic frequencies ω_e, anharmonic corrections $\omega_e x_e$, and equilibrium bond distances r_e have been obtained through a standard Dunham analysis.[55]

All calculations were done under C_{2v} symmetry restrictions with the MOLPRO 2012 package of programs.[56]

III. RESULTS AND DISCUSSION

Table I collects the molecular parameters for the $X^1\Sigma^+$, $^3\Pi_{A'2}$, and $^3\Pi_{A1}$ states at the valence and CV MRCI(+Q) and RCCSD(T) levels of theory while Table II gathers the molecular parameters for all bound states presently studied or for states that display local minima sustaining some vibrational levels along with the corresponding experimental values. Figures 1–4 display the corresponding PECs. In what follows we offer a succinct discussion of their electronic structure presented according to their adiabatic separation limits. We tag the states as $^{2S+1}\Lambda_\Omega$, a letter alluding to its spectroscopic notation precedes the quantum number Ω.

A. States correlating to two ground ^2P atomic fragments

Two ground state atomic fragments in the LS coupling limit (^2P) give rise to $12 \ ^{2S+1}\Lambda$ molecular states of $(^{1,3}\Sigma^+[2],^{1,3}\Sigma^-,^{1,3}\Pi[2],^{1,3}\Delta)$ spatial and spin symmetry (see the inset plot of Fig. 1). Disregarding for the moment the large SO effects that cause the ΛS symmetries inappropriate for the study of its electronic spectroscopy we would like to give some insights on the bonding nature of the above states based on the traditional and chemically intuitive valence bond Lewis (vbL) structures.

The two Σ^+ and Σ^- states result from the combination$|^2P, \ M_L = 0, \ \pm1, \ \pm1\rangle_I \otimes \ |^2P, \ M_L = 0, \ \mp1, \ \mp1\rangle_{Cl}$, respectively. It is rather straightforward to understand that only the $(0,0)$ combination will result in a chemically bound system while the $(\pm1, \mp1)$ combinations of $\Sigma^\pm$ symmetries will be unbound. Pictorially we have the following vbL icon for the $\sigma-$bonded $^1\Sigma^+$ state resulting from the $(0, 0)$ fragments,
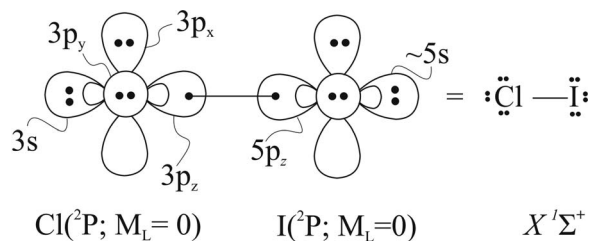

Cl(^2P; $M_L= 0$)   I(^2P; $M_L=0$) $X \, ^1\Sigma^+$

TABLE I. Energies E (E$_h$), bond distances r$_e$ (Å), harmonic frequencies ω_e, anharmonic corrections $\omega_e x_e$ (cm^{-1}), dissociation energies D$_e$ (kcal/mol), and excitation energies T$_e$ (cm^{-1}) of the $X^1\Sigma^+$, $^3\Pi_{A'2}$, and $^3\Pi_{A1}$ I^{35}Cl states at various levels of theory.

State	Method	−E	r$_e$	ω_e ($\omega_e x_e$)	D$_e$	T$_e$
$X^1\Sigma^+$	MRCI[a]	754.556 000	2.330	388.01 (1.432)	52.81	0.0
	MRCI+Q[a]	754.600 045	2.332	388.10 (1.406)	54.20	0.0
	RCCSD(T)[a]	754.611 238	2.324	393.92 (1.380)	55.5	0.0
	C-MRCI[b]	755.040 147	2.319	389.55 (1.467)	51.74	0.0
	C-MRCI+Q[b]	755.150 741	2.316	392.17 (1.338)	54.05	0.0
	C-RCCSD(T)[b]	755.200 417	2.314	395.93 (1.416)	55.70	0.0
	C-MRCI[c]	755.372 692	2.319	391.45 (1.603)	51.84	0.0
	C-MRCI+Q[c]	755.526 380	2.313	395.97 (1.504)	54.66	0.0
	C-RCCSD(T)[c]	755.597 180	2.314	396.41 (1.376)	55.70	0.0
	Expt.[d]		2.320 85	384.30 ± 0.02 (1.501 ± 0.006)	50.20 ± 0.29	
$^3\Pi_{A'2}$	C-MRCI+SO[b]	754.978 105	2.768	158.13 (3.640)	4.90	13 617
	C-MRCI+SO+Q[b]	755.092 863	2.717	186.62 (3.324)	9.67	12 703
	C-MRCI+SO[c]	755.309 352	2.793	146.40 (3.653)	4.06	13 902
	C-MRCI+SO+Q[c]	755.466 251	2.732	175.55 (3.039)	8.77	13 197
	Expt.[e]		2.665(1)	224.57 (1.882)	13.94 ± 0.08	12 682.05
$^3\Pi_{A1}$	C-MRCI+SO[b]	754.974 204	2.831	125.62 (5.624)	2.45	14 473
	C-MRCI+SO+Q[b]	755.088 679	2.758	160.85 (3.714)	7.04	13 621
	C-MRCI+SO[c]	755.305 625	2.873	107.37 (6.165)	1.72	14 720
	C-MRCI+SO+Q[c]	755.462 174	2.780	147.86 (3.831)	6.22	14 092
	Expt.[d]		2.676 96	210.3 ± 0.1 (1.50 ± 0.07)	10.91 ± 0.11	13 742.92 ± 0.06

[a]Valence (5s^{2}5p^5 + 3s^{2}3p^5 e$^-$) calculations with the [cc-pwCV5Z-PP/$_I$ cc-pwCV5Z/$_{Cl}$] basis set.
[b]Core-valence (4d^{10}5s^{2}5p^5 + 3s^{2}3p^5 e$^-$) calculations with the [cc-pwCV5Z-PP/$_I$ cc-pwCV5Z/$_{Cl}$] basis set.
[c]Core-valence (4s^{2}4p^{6}4d^{10}5s^{2}5p^5 + 3s^{2}3p^5 e$^-$) calculations with the [cc-pwCV5Z-PP/$_I$ cc-pwCV5Z/$_{Cl}$] basis set.
[d]Reference 18.
[e]Reference 15.

The second $^1\Sigma^+$ state dissociating to the (± 1, ∓1) combination of two rather dissimilar ($\langle r \rangle_{5p}/\langle r \rangle_{3p} = 1.36$[57]) atoms does not allow any bonding interaction, the same also holds true for the Σ^- and Δ (± 1, ± 1) symmetries. The Π states result from either the (0, ± 1) or the (± 1, 0) atomic combinations offering the possibility for two $3e^- - 2$ c(enter) bonds with the $^3\Pi$ state being substantially bound while its singlet analog is of quasi bound character. So, within the ΛS scheme only two states, the $^1\Sigma^+$ and the $^3\Pi$, are bound while the rest 10 $^{2S+1}\Lambda$ states are repulsive; see the inset of Fig. 1. The inclusion of the SO effects changes completely the morphology of most of the PECs as can be seen in Fig. 1, revealing a number of bound states not present in the ΛS energy scheme. All $^{2S+1}\Lambda$ states dissociating to two ground state ^{2}P atoms have been state averaged at the CASSCF level thus creating a common set of molecular orbitals. For all these ±Λ states we have calculated the MRCI wavefunctions which were used in the construction and diagonalization of the SO Hamiltonian matrix (36 × 36). Two sets of MRCI and MRCI+SO calculations were done for the same set of $^{2S+1}\Lambda$ and Ω states differing in the size of the reference space employed for the generation of the single and double excitations. In the first set of calculations the internal space of the CI resulted from the distribution of 14 (7 + 7) e^- in 8 (3s + 3p + 5s + 5p) valence orbitals giving rise to 5.7 × 10^6 (^{1}A$_1$), 2.7 × 10^6 (^{1}A$_2$), 3.8 × 10^6 (^{1}B$_1$), 8.0 × 10^6 (^{3}A$_1$), 4.6 × 10^6 (^{3}A$_2$), and 6.4 × 10^6 (^{3}B$_1$) CFs. In the second set of calculations the 14 valence electrons were distributed in the space of 8 + 5 = 13 active orbitals, the additional 5 orbitals of primarily d(Cl) character were determined at the CI level for states of ^{1}A$_1$ symmetry.

The "*augmented*" MRCI(*aug*) spaces consist of 692 × 10^6 (^{1}A$_1$, ^{1}A$_2$, and ^{1}B$_1$), and 1.3 × 10^9 (^{3}A$_1$, ^{3}A$_2$, and ^{3}B$_1$) CFs. That way we give more correlation space to the already congested Hartree–Fock 3s^{2}3p^5 electronic cloud at the level of reference space providing better energetic results.

Let us consider first the atomic splittings between the 3/2 and 1/2 J components of the ^{2}P term. The experimental values[52] are $\Delta E_{Cl}(1/2 \leftarrow 3/2) = 882.3515$ cm^{-1} and $\Delta E_I(1/2 \leftarrow 3/2) = 7602.970$ cm^{-1} while the corresponding theoretical values are 810 (800) and 7062 (7020) cm^{-1} with the valence (augmented) active spaces, respectively, no more than 8% off the experimental values.

It is interesting to present in some detail the results of the $X^1\Sigma^+$ state of I^{35}Cl, a state that is the least "perturbed" by the SO effects. We will firstly comment on the CV correlation effects. We have considered in a step by step basis the effect of the 4d^{10} (Table I), 4s^{2}4p^{6}4d^{10} (Table I) and 4s^{2}4p^{6}4d$^{10}/_I$ + 2s^{2}2p$^6/_{Cl}$ (Table II) electrons at both the MRCI(+SO), MRCI(+SO+Q) and RCCSD(T) levels of theory. The combined effects of missing electronic correlation and size non-extensivity "errors" with respect to the RCCSD(T) results are pretty large even at the valence correlation level (55 mE$_h$) graciously corrected at the +Q level of theory; the remaining "error" is ∼ 11 mE$_h$ (see Table I). When including the 4d^{10} electrons the MRCI "error" amounts to 160 mE$_h$ while at the MRCI+Q level to ∼50 mE$_h$. By considering the entire n = 4 shell, the MRCI "error" is 224 mE$_h$ and the MRCI+Q one is 71 mE$_h$. In the light of the above results we should be extreme cautious when interpreting the CV results. At the valence level the equilibrium distance r$_e$ is pretty large, i.e.,

TABLE II. Energies E (E_h), bond distances r_e (Å), harmonic frequencies ω_e, anharmonic corrections $\omega_e x_e$ (cm^{-1}), dissociation energies D_e (kcal/mol) and excitation energies T_e (cm^{-1}) of fourteen I^{35}Cl states at various levels of theory.

State	Method	−E	r_e	ω_e ($\omega_e x_e$)	D_e	T_e
$X^1\Sigma_{0^+}^+$	MRCI	754.551 756	2.332	387.55 (1.457)	50.6	0.0
	MRCI+Q	754.599 293	2.332	389.71 (1.775)	54.0	0.0
	MRCI(aug)[a]	754.580 295	2.324	396.23 (1.455)	53.8	0.0
	MRCI(aug)[a]+Q	754.599 294	2.279	390.03 (1.689)	49.0	0.0
	RCCSD(T)[b]	754.611 238	2.324	393.92 (1.380)	55.5	0.0
	C-RCCSD(T)[c]	755.597 180	2.314	396.41 (1.376)	55.7	0.0
	C-RCCSD(T)[d]	755.941 281	2.311	397.46 (1.381)	55.8	0.0
	MRCI+SO	754.554 093	2.339	379.01 (1.481)	44.6	0.0
	MRCI(aug)[a]+SO	754.582 744	2.331	387.48 (1.416)	48.0	0.0
	MRCI(aug)[a] +SO+Q	754.609 859	2.336	383.26 (1.539)	49.7	0.0
	Expt.[e]		2.320 85	384.30 ± 0.02 (1.501 ± 0.006)	50.20 ± 0.29	0.0
$^3\Pi_{A'2}$	MRCI+SO	754.494 748	2.731	183.97 (2.656)	7.35	13 025
	MRCI(aug)[a]+SO	754.519 126	2.713	204.53 (2.022)	8.03	13 963
	MRCI(aug)[a]+SO+Q	754.552 146	2.676	220.31 (2.767)	13.44	12 667
	Expt.[f]		2.665(1)	224.57 (1.882)	13.94 ± 0.08	12 682.05
$^3\Pi_{A1}$	MRCI+SO	754.490 467	2.770	159.91 (3.383)	4.65	13 964
	MRCI(aug)[a]+SO	754.514 502	2.739	185.20 (2.704)	5.13	14 977
	MRCI(aug)[a]+SO+Q	754.547 090	2.674	201.21 (0.966)	10.28	13 776
	Expt.[e]		2.676 96	210.3 ± 0.1 (1.50 ± 0.07)	10.91 ± 0.11	13 742.92 ± 0.06
$^3\Pi_{0^-}$	MRCI(aug)[a]+SO	754.504 362	2.820			17 203
	MRCI(aug)[a]+SO+Q	754.536 493	2.781	186.07 (5.448)	3.63	16 102
$^3\Pi_{B0^+}$	MRCI(aug)[a]+SO	754.499 614	2.738			18 245
	MRCI(aug)[a]+SO+Q	754.532 178	2.680	214.48 (16.45)	0.93	17 049
	Expt.[e]		2.611 78	211.42 ± 0.03 (7.976 ± 0.007)	0.52 ± 0.06	17 376.04 ± 0.05
$^3\Sigma_{B'0^+}^-$	MRCI(aug)[a]+SO	754.503 46	~4.02			17 400
	Expt.[e]			36.855 ± 0.4 (1.135 ± 0.1)	0.65 ± 0.06	18 157.1 ± 0.02
$^3\Pi_{B''0^+}$	MRCI+SO	754.456 637	3.174	141.63 (4.983)	3.60	21 389
	MRCI(aug)[a]+SO	754.479 313	3.182	140.69 (4.852)	3.12	22 700
$^3\Pi_{D'2}$	MRCI+SO	754.369 142	3.386	172.94 (0.399)	86.2	40 594
	MRCI+SO+Q	754.430 130	3.366	174.68 (0.449)	100	39 446
	Expt.[g]		3.3502	173.63 (0.5572)	96.2	39 061.83
	Local minimum					
	MRCI+SO	754.314 674	2.241	440.73 (1.383)		52 546
	MRCI+SO+Q	754.359 272	2.234	443.96 (0.837)		54 998
	Expt.[h, i]					53 500
$^3\Pi_{\beta1}$	MRCI+SO	754.357 462	3.380	173.59 (0.374)	85.5	43 157
	MRCI+SO+Q	754.418 459	3.360	174.45 (0.341)	99.3	42 007
	Expt.[g]		3.2930	170.31 (0.4706)	96.1	39 103.67
	Local minimum					
	MRCI+SO	754.304 310	2.248	423.71 (−2.014)		54 821
	MRCI+SO+Q	754.349 253	2.229	446.32 (1.756)		57 196
	Expt.[i]					58 197
$^3\Sigma_{f0^+}^-$	MRCI	754.350 654	3.185	181.28 (0.706)	81.4	44 136
	MRCI+Q	754.419 840	3.136	184.85 (1.113)	100.6	39 386
	Expt.[j]		3.2582	184.158 (0.7439)	98.0	44 924.375
$^3\Pi_{E0^+}$	MRCI+SO	754.345 766	3.374	173.57 (0.304)	78.1	45 724
	MRCI+SO+Q	754.406 781	3.354	175.48 (0.423)	92.0	44 570
	Expt.[g]		3.2553	165.69 (0.288)	96.2	39 059.48
	Local minimum					
	MRCI+SO	754.294 832	2.238	438.04 (0.508)		56 901
	MRCI+SO+Q	754.339 531	2.227	447.37 (1.704)		59 330
	Expt.[i]					57 557
$^1\Sigma_{f'0^+}^+$	MRCI	754.321 462	3.292	162.0 (0.202)	70.6	50 543
	MRCI+Q	754.383 302	3.250	161.12 (−0.813)	83.8	47 404
	Expt.[k]			160.72 (0.195)	100.9	51 199.96

TABLE II. (*Continued.*)

State	Method	−E	r_e	ω_e ($\omega_e x_e$)	D_e	T_e
$^1\Delta$	MRCI	754.316 432	3.158	183.56 (0.607)	67.5	51 647
	MRCI+Q	754.379 052	3.124	186.03 (0.367)	81.2	48 337
$^1\Pi_{H'1}$	MRCI	754.315 712	3.300	183.30 (0.612)	66.7	52 319
	MRCI+Q	754.379 811	3.283	184.06 (0.502)	81.6	48 171
	Expt.[k]			184.03 (0.596)		51 615.6
	Local minimum					
	MRCI	754.295 843	2.238	445.01 (1.344)		56 679
	MRCI+Q	754.343 212	2.234	455.81 (2.129)		56 203

[a]MRCI calculations using the "*augmented*" reference space, see text for details.
[b]Valence $(5s^2 5p^5 + 3s^2 3p^5\ e^-)$ RCCSD(T)/[cc-pwCV5Z-PP/$_I$ cc-pwCV5Z/$_{Cl}$] calculations.
[c]Core-valence $(4s^2 4p^6 4d^{10} 5s^2 5p^5 + 3s^2 3p^5\ e^-)$ RCCSD(T)/[cc-pwCV5Z-PP/$_I$ cc-pwCV5Z/$_{Cl}$] calculations.
[d]Core-valence $(4s^2 4p^6 4d^{10} 5s^2 5p^5 + 2s^2 2p^6 3s^2 3p^5\ e^-)$ RCCSD(T)/[cc-pwCV5Z-PP/$_I$ cc-pwCV5Z/$_{Cl}$] calculations.
[e]Reference 18.
[f]Reference 15.
[g]References 44 and 60.
[h]Reference 33.
[i]Reference 31.
[j]Reference 32 and D_e from Ref. 29.
[k]Reference 34.

r_e(MRCI) = 2.330 Å while at the RCCSD(T) level of theory (r_e = 2.324 Å) it gets much closer to the experimental value of r_e = 2.320 85 Å.[18] The situation is also good at the C-MRCI($4d^{10}$) level of theory with an obtained value of r_e = 2.319 Å, but r_e tends to become even smaller at the C-MRCI($4d^{10}$)+Q (r_e = 2.316 Å), C-RCCSD(T)($4d^{10}$) (r_e = 2.314 Å), C-MRCI($4s^2 4p^6 4d^{10}$)+Q (r_e = 2.313 Å) and C-RCCSD(T)($4s^2 4p^6 4d^{10}$ and $4s^2 4p^6 4d^{10} + 2s^2 2p^6$) ($r_e$ = 2.314 and 2.311 Å) levels of theory. We do not observe any dramatic differences in the ω_e($\omega_e x_e$) values. One remark though seems to be in order. At both the valence and CV
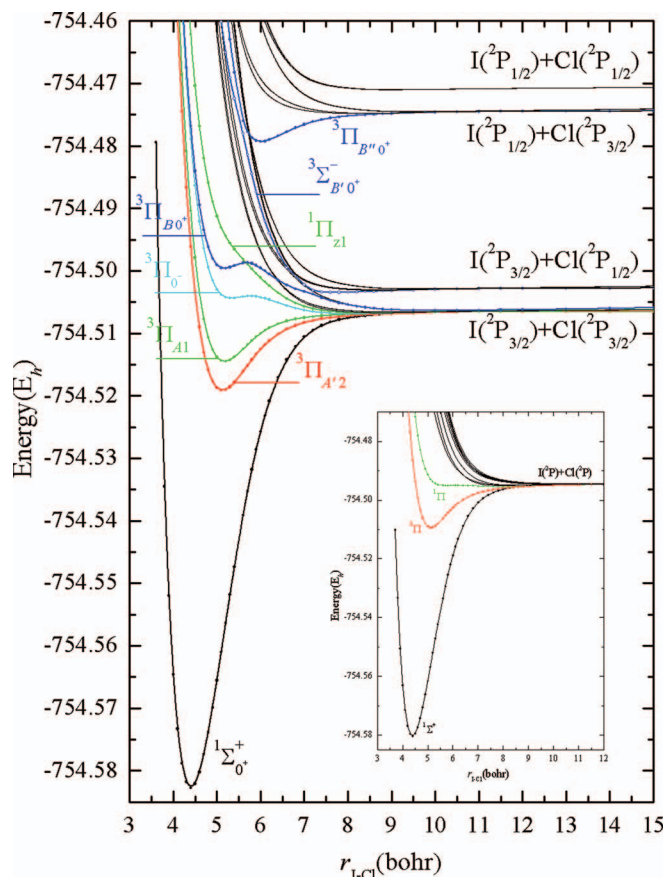

FIG. 1. MRCI+SO energy curves of all Ω ICl states dissociating to two ground state atoms I(^{2}P$_{1/2,3/2}$) + Cl(^{2}P$_{1/2,3/2}$). The inset displays the MRCI energy curves of all $^{2S+1}\Lambda$ ICl states dissociating to I(^{2}P) + Cl(^{2}P). Energy ranges from 0 to 26 940 cm^{-1}.
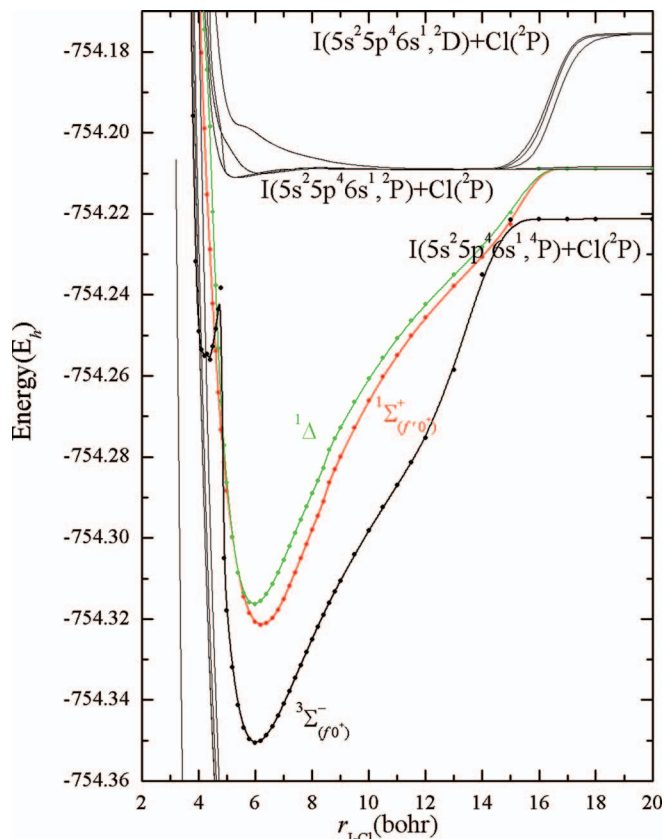

FIG. 2. MRCI energy curves of the $^3\Sigma^-$, $^1\Sigma^+$, and $^1\Delta$ ICl states dissociating to I($5s^2 5p^4 6s^1$; ^{4}P) + Cl(^{2}P). Energy extends from 48 887 to 90 587 cm^{-1}.
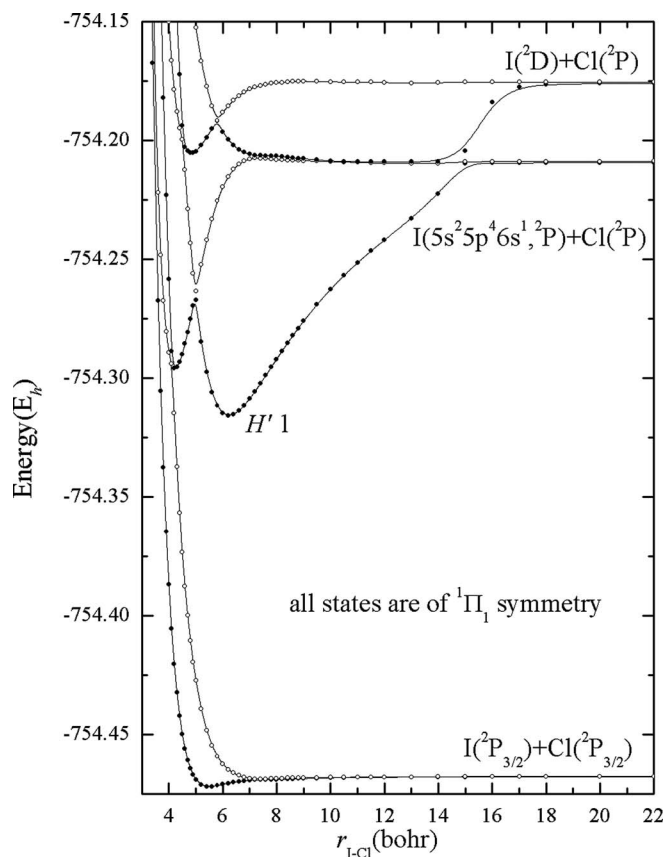
FIG. 3. MRCI energy curves of six $^1\Pi$ ICl states dissociating to various asymptotic channels; see text for details. Energy extends from 23 647 to 94 976 cm^{-1}.
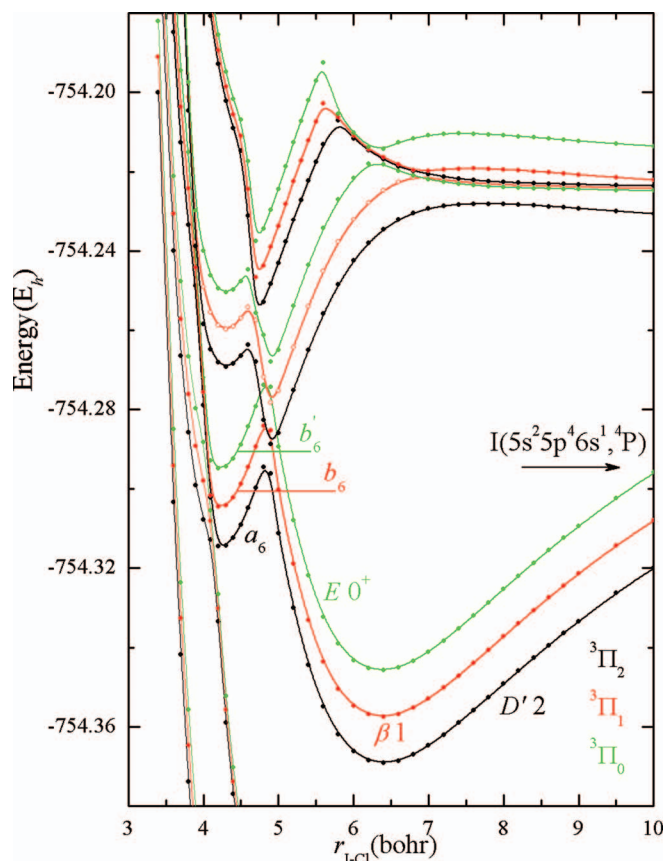

FIG. 4. MRCI+SO energy curves of three $^3\Pi_{2,1,0}$ ICl states dissociating to various asymptotic channels; see text for details. Energy extends from 44 497 to 88 392 cm^{-1}.

RCCSD(T) levels the above molecular parameters are systematically found to be larger than the MRCI ones and this is due to the fact that the RCCSD(T) method being unable to correctly dissociate the molecular states produces steeper PECs.

At the MRCI(+Q)[SO]{exp}[18] level the equilibrium properties of the X state are E = $-754.551\,756$ ($-754.599\,293$) [$-754.554\,093$] E$_h$, r$_e$ = 2.332 (2.332) [2.339] {2.320 85} Å, ω_e = 387.5 (389.7) [379.0] {384.30 $\pm$ 0.02} cm^{-1} and D$_e$ = 50.6 (54.0) [44.6] {50.20 $\pm$ 0.29} kcal/mol with the valence reference space while with the "*augmented*" reference space the results are E = $-754.580\,295$ ($-754.599\,294$) [$-754.582\,744$] E$_h$, r$_e$ = 2.324 (2.279) [2.331] {2.320 85} Å, ω_e = 396.2 (390.0) [387.5] {384.30 $\pm$ 0.02} cm^{-1}, and D$_e$ = 53.8 (49.0) [48.0] {50.20 $\pm$ 0.29} kcal/mol; see Table II. Although the MRCI energy drop due to the additional five "d" orbitals is $\sim$30 mE$_h$ the molecular parameters seem to be rather insensitive with the exception of the D$_e$ value at the MRCI+SO level of theory (48.0 *vs* 44.6 kcal/mol) which is closer to the experimental one (50.20 kcal/mol). The SO effects amount to only 2.4 mE$_h$ at both reference spaces, an energy contribution due to the small (2%) presence of the first but rather remote $^3\Pi$ state (ΔE($^3\Pi \leftarrow {}^1\Sigma^+$) = 44.5 kcal/mol).

The first excited state is of $^3\Pi$ symmetry giving rise to 0^+, 0^-, 1, and 2 Ω states, all of them dissociating to two ground state atoms, i.e., $|^2P_{3/2}\rangle_I \otimes |^2P_{3/2}\rangle_{Cl}$. The $^3\Pi$ state is

bound by 9.3 kcal/mol due to two $3e^- - 2c$ bonds, a σ and a π. The analysis of the equilibrium MRCI+SO wavefunctions is quite revealing,

$$\left|^3\Pi_{\Omega=2}\right\rangle \cong 0.50\left[\left|^3\Pi_x, \Sigma=1\right\rangle + i\left|^3\Pi_y, \Sigma=1\right\rangle\right]$$
$$+ 0.50\left[\left|^3\Pi_x, \Sigma=-1\right\rangle - i\left|^3\Pi_y, \Sigma=-1\right\rangle\right],$$

$$\left|^3\Pi_{\Omega=1}\right\rangle \cong 0.92\left|^3\Pi, \Sigma=0\right\rangle + 0.37\left|^1\Pi, \Sigma=0\right\rangle,$$

$$\left|^3\Pi_{\Omega=0^-}\right\rangle \cong 0.50\left[\left|^3\Pi_x, \Sigma=1\right\rangle - i\left|^3\Pi_y, \Sigma=1\right\rangle\right]$$
$$- 0.50\left[\left|^3\Pi_x, \Sigma=-1\right\rangle + i\left|^3\Pi_y, \Sigma=-1\right\rangle\right],$$

$$\left|^3\Pi_{\Omega=0^+}\right\rangle \cong 0.50\left[\left|^3\Pi_x, \Sigma=1\right\rangle - i\left|^3\Pi_y, \Sigma=1\right\rangle\right]$$
$$+ 0.50\left[\left|^3\Pi_x, \Sigma=-1\right\rangle + i\left|^3\Pi_y, \Sigma=-1\right\rangle\right],$$

alluding to the purity of the Ω states, i.e., being practically of only $^3\Pi$ spatial-spin symmetry. For the first excited and experimentally "dark" (A') $^3\Pi_2$ state, the MRCI(*augmented*)+SO+Q valence results of I^{35}Cl are, r$_e$ = 2.676 Å, ω_e = 220 cm^{-1}, $\omega_e x_e$ = 2.767 cm^{-1}, D$_e$ = 13.44 kcal/mol, and T$_e$ = 12 667 cm^{-1}, while the limited experimental data are r$_e$ = 2.63,[11] 2.665(1)[15] Å, ω_e = 226(4),[11] 224.57(15)[15] cm^{-1}, $\omega_e x_e$ = 1.394,[11] 1.882[15] cm^{-1}, D$_e$ = 13.95 $\pm$ 0.06,[11] 13.94 $\pm$ 0.08[15] kcal/mol, and T$_e$ = 12 680(20),[11] 12 682.05(27)[15] cm^{-1}. The agreement is

indeed excellent. At the C-MRCI(+Q) level of theory when correlating either the $4d^{10}$ or $4s^2 4p^6 4d^{10}$ electrons the results are not good; see Table I, due to the severe size non-extensivity errors discussed earlier and the lack of the additional five "d" orbitals in the reference space at the CI level.

The second excited state is the $\Omega = 1$ (A) component of $^3\Pi$ and the only one from this set that is a mixture of 84% $^3\Pi(\Sigma = 0)$ and of 14% $^1\Pi(\Sigma = 0)$. Our theoretical valence MRCI(*augmented*)+SO+Q values are $r_e = 2.674$ Å, $\omega_e = 201$ cm^{-1}, $\omega_e x_e = 0.966$ cm^{-1}, $D_e = 10.28$ kcal/mol, and $T_e = 13\,776$ cm^{-1}. The corresponding experimental values are $r_e = 2.676\,96$,[18] 2.685,[15] 2.685(1)[9] Å, $\omega_e = 210.3 \pm 0.1$,[18] 211.0,[15] 211.0(3)[9] cm^{-1}, $\omega_e x_e = 1.50 \pm 0.07$,[18] 2.12,[15] 2.12(1)[9] cm^{-1}, $D_e = 10.91 \pm 0.11$,[18] 10.91[15,9] kcal/mol, and $T_e = 13\,742.92 \pm 0.06$,[18] 13\,742.9,[15] 13\,742.9(5)[9] cm^{-1} in excellent agreement with the obtained theoretical values. As can be seen in Fig. 1, there are three more states of potential interest that are either bound with respect to their dissociation limit or present local minima, the rest are of repulsive nature and will not be considered any further. The $^3\Pi(\Omega = 0^+)$ state presents a local minimum at 2.680 Å with $\omega_e = 214.5$ cm^{-1}, $\omega_e x_e = 16.45$ cm^{-1} $D_e = 325.3$ cm^{-1} and an excitation energy of $T_e = 17\,049$ cm^{-1} only at the augmented MRCI+SO+Q level of theory, the morphology of its PEC at the valence space (without the d orbitals) is smoother with no minimum. The latest experimental data[18] on the (B) 0^+ state are $r_e = 2.611\,78$ Å, $\omega_e = 211.42 \pm 0.03$ cm^{-1}, $\omega_e x_e = 7.976 \pm 0.007$ cm^{-1}, $D_e = 183 \pm 20$ cm^{-1},[58] and $T_e = 17\,376.04 \pm 0.05$ cm^{-1} in very good agreement with the calculated values.

The last state to be discussed is of (B'') 0^+ symmetry and dissociates adiabatically to I($^2P_{1/2}$) + Cl($^2P_{3/2}$). At the equilibrium distance its wavefunction is an amalgam of four different ΛS states, i.e.,

$$|0^+\rangle \cong 0.36|X^1\Sigma^+\rangle + 0.24|3^1\Sigma^+\rangle$$
$$+ 0.31\left[|1^3\Pi_x, \Sigma = 1\rangle - i\,|1^3\Pi_y, \Sigma = 1\rangle\right]$$
$$+ 0.32\left[|2^3\Pi_x, \Sigma = 1\rangle - i\,|2^3\Pi_y, \Sigma = 1\rangle\right]$$
$$+ 0.31\left[|1^3\Pi_x, \Sigma = -1\rangle + i\,|1^3\Pi_y, \Sigma = -1\rangle\right]$$
$$+ 0.32\left[|2^3\Pi_x, \Sigma = -1\rangle + i\,|2^3\Pi_y, \Sigma = -1\rangle\right],$$

with molecular constants $r_e = 3.174(3.182)$ Å, $\omega_e = 142(141)$ cm^{-1}, $\omega_e x_e = 4.98(4.85)$ cm^{-1}, $D_e = 3.60$ (3.12) kcal/mol, and $T_e = 21\,389(22\,700)$ cm^{-1} at the valence (*augmented*) MRCI+SO level of theory. It is an experimentally undetected state but termed as B'' in Ref. 14.

A last comment on the avoided crossings between the $^3\Pi_{B0^+}$ and $^3\Sigma^-_{B'0^+}$ and $^3\Sigma^-_{B'0^+}$ and $^3\Pi_{B''0^+}$ states (see Fig. 1) is in order since they are predicted to contribute to the absorption bands of the UV photodissociation spectra of ICl.[40–42] Tonokura *et al.*[42(a)] have found these avoided crossings at 7.05 and 5.4 bohrs, respectively, more recently Yabushita and co-workers[42(b), 42(d)] have placed them at 6.84 and 5.38 bohrs, respectively, while we have found them at 7.2 and 5.6 bohrs, respectively. Such differences could in general be significant in the theoretical simulations of the photodissociation dynamics of the ICl;

however, we should note that apart of their positions, the non-adiabatic coupling terms, as well as their whole shape, especially in the long-range region,[43] of the underlying PECs have be found[42(c), 43] to play a more significant role. In addition, quantum interference effects between the states produced by the coherent excitation during the photodissociation,[59] have also been found[42(d)] to influence the comparison between theoretical calculations and experimental data. Such investigation, involving non-adiabatic quantum dynamics simulations, is beyond the scope of the present article, and thus, it is not possible to comment meaningfully on the relevance of the calculated PECs on the experimental measurements of the photofragment branching ratios, angular momentum polarization, and anisotropy parameters of the ICl.

B. States correlating to a Rydberg I atom

The states to be discussed in this paragraph correlate adiabatically to an I atom of Rydberg nature. Based on preliminary calculations at the CASSCF level of theory we have constructed MRCI PECs for states of $^1\Sigma^+$, $^1\Delta$, $^3\Sigma^-$ (Fig. 2), $^1\Pi[4]$ (Fig. 3), and $^3\Pi[3]$ (Fig. 4) symmetry "corrected" for by only the diagonal SO effects.

The lowest lying state displayed in Fig. 2 is of $^3\Sigma^-$ symmetry giving rise to $\Omega = 0^+$ and 1 states upon second order SO effects. Although the $^3\Sigma^-$ state correlates adiabatically to I($5s^2 5p^4(^3P)6s^1$, ^4P) + Cl($3s^2 3p^5$, ^2P) it originates from the ionic limit I$^+$($5s^2 5p^4$, ^3P) + Cl$^-$($3s^2 3p^6$, ^1S) due to a severe avoided crossing at 15.0 bohr. This ionic limit generates six Ω states, which according to Hund's case c are designated as $0^+(^3P_2)$, $1(^3P_2)$, $2(^3P_2)$, $0^-(^3P_1)$, $1(^3P_1)$, and $0^+(^3P_0)$. The CASSCF equilibrium CFs are (showing only 10 valence electrons)

$$|^3\Sigma^-\rangle \cong 0.87\left|1\sigma^2(2p_z^{Cl})2\sigma^2(2p_z^I)1\pi_x^2(2p_x^{Cl})2\pi_x^1(2p_x^I)1\pi_y^2\right.$$
$$\times\left.(2p_y^{Cl})2\pi_y^1(2p_y^I)\right\rangle$$
$$+ 0.27\left|1\sigma^2 2\sigma^2\left(1\pi_x^2 2\pi_x^1 1\pi_y^1 2\pi_y^2 + 1\pi_x^1 2\pi_x^2 1\pi_y^2 2\pi_y^1\right)\right\rangle,$$

with Mulliken atomic charges of I$^{+0.84}$Cl$^{-0.84}$, both of them being typical for an ion-pair state. The MRCI(+Q) molecular constants of its adiabatic PEC are $r_e = 3.185$ (3.136) Å, $\omega_e = 181.3$ (184.9) cm^{-1}, $\omega_e x_e = 0.706$ (1.113) cm^{-1}, $D_e = 81.4$ (100.6) kcal/mol, and $T_e(^3\Sigma^- \leftarrow X^1\Sigma^+) = 44\,136$ (39\,386) cm^{-1}. Although the $^3\Sigma^-$ state can be viewed as a potential perturber to the (E)$^3\Pi_{0^+}$ state the above molecular constants are in very good agreement with the constants of the $f\,0^+(^3P_0)$ state, i.e., $r_e = 3.2582(3)$ Å,[32] $\omega_e = 184.40(16)$,[29] 184.158(8)[32] cm^{-1}, $\omega_e x_e = 0.771(19)$,[29] 0.7439(15)[32] cm^{-1}, $D_e = 98.0$ kcal/mol,[29] and $T_e = 44\,923.79(41)$,[29] 44\,924.375(29)[32] cm^{-1}, observed for the first time by Brand *et al.*,[29] in 1984. A $^3\Sigma^-$ state appears in the literature as a diabatic component in a post Born–Oppenheimer treatment of the $^3\Pi$, $^3\Sigma^-$, and $^1\Sigma^+$ states that correlate to I$^+$(^3P, ^1D) + Cl$^-$(^1S), a treatment that aims to model the ion-pair $0^+(^3P_2, ^3P_0)$ and $1(^3P_2, ^3P_1)$ states.[44]

Two more states of $^1\Sigma^+_{(0^+)}$ and $^1\Delta_{(2)}$ $\Lambda S_{(\Omega)}$ symmetry appear in Fig. 2 that correlate adiabatically to I($5s^2 5p^4(^3P)6s^1$, ^2P) + Cl($3s^2 3p^5$, ^2P) but they are of ion-pair character due to

an avoided crossing at 16.0 bohr with states originating from $I^+(5s^25p^4, \,^1D) + Cl^-(3s^23p^6, \,^1S)$ through intermediate states correlating to $I(5s^25p^46s^1, \,^2D) + Cl(3s^23p^5, \,^2P)$.

The $^1\Sigma_{(0^+)}^+$ state can be identified with the f' $0^+(^1D_2)$ state observed through double-resonance ionization nozzle-cooled spectroscopy for the first time by Donovan *et al.*[34] in 1993. The limited available experimental data[34] T_e = 51 199.96 cm^{-1}, ω_e = 160.72 cm^{-1}, $\omega_e x_e$ = 0.195 cm^{-1}, and D_e = 100.9 kcal/mol are in good agreement with the MRCI(+Q) molecular constants r_e = 3.292 (3.250) Å, ω_e = 162.0 (161.1) cm^{-1}, $\omega_e x_e$ = 0.202 (−0.813) cm^{-1}, T_e = 50 543 (47 404) cm^{-1} and D_e = 70.6(83.3) kcal/mol. Its equilibrium CASSCF CFs is an amalgam of different configurations,

$$|^1\Sigma^+\rangle \cong \left|[(0.63)1\sigma^2 + (0.57)1\sigma^12\bar{\sigma}^1]1\pi_x^22\pi_x^21\pi_y^22\pi_y^2\right\rangle$$
$$+0.35\left|[1\sigma^22\sigma^21\pi_x^21\pi_y^2(2\pi_x^2 + 2\pi_y^2)\right\rangle,$$

while the Mulliken atomic charges $I^{+0.83}Cl^{-0.83}$ conform to its ion-pair nature. It is also true that the E 0^+ $(^3\Pi_{0^+})$, $f\,0^+(^3P_0)$, and f' $0^+(^1D_2)$ states would form a 3×3 non-adiabatic system for the calculation of the vibrational levels as postulated by Donovan *et al.*[34]

The highest lying state in Fig. 2 is of $^1\Delta$ symmetry giving rise to a $\Omega = 2$ state upon SO interaction. To the best of our knowledge a $2(^1D_2)$ ion-pair state has never been observed before. The equilibrium CASSCF CFs are typical for a $\Lambda = 2$ symmetry,

$$|^1\Delta\rangle \cong 0.68\left|1\sigma^22\sigma^21\pi_x^21\pi_y^2(2\pi_x^2 - 2\pi_y^2)\right\rangle,$$

with Mulliken atomic charges of $I^{+0.90}Cl^{-0.90}$, mirroring the ionic character due to the $I^+(^1D, \, M_L = \pm2)$ atomic term. Its MRCI(+Q) molecular parameters are r_e = 3.158 (3.124) Å, ω_e = 183.6 (186.0) cm^{-1}, $\omega_e x_e$ = 0.607 (0.367) cm^{-1}, D_e = 67.5(81.2) kcal/mol, and T_e = 51 647 (48 337) cm^{-1}.

The last states to be discussed are of $^3\Pi$ and $^1\Pi$ ΛS symmetry correlating adiabatically to $I(5s^25p^46s^1, \,^4P) + Cl(^2P)$ and $I(5s^25p^46s^1, \,^2P) + Cl(^2P)$, respectively, but diabatically to the ion-pair fragments $I^+(^3P) + Cl^-(^1S)$ and $I^+(^1D) + Cl^-(^1S)$, respectively. We have constructed PECs of five $^3\Pi$ and six $^1\Pi$ states correlating to $I(5s^25p^5, \,^2P)$ [$^3\Pi(2)$ and $^1\Pi(2)$], $I(5s^25p^46s^1, \,^4P)$ [$^3\Pi(2)$], $I(5s^25p^46s^1, \,^2P)$ [$^3\Pi$ and $^1\Pi(2)$], and to $I(5s^25p^46s^1, \,^2D)$ [$^1\Pi(2)$].

The $^1\Pi$ symmetry gives rise only to $\Omega = 1$ states while the $^3\Pi$ one to states of $\Omega = 0^+, 0^-, 1$, and 2. We have considered only the diagonal form of the SO operator, thus the $^1\Pi$ PECs remained identically the same while the $^3\Pi$ ones were split into the $\Omega = 2, 1$, and 0 (the $\pm$ symmetry could not be differentiated) components equidistantly separated by $\Delta E(1\leftarrow2) = \Delta E(0\leftarrow1) = 12$ mE_h. Needless to say that the same happens for the $^3\Pi$ state correlating to two ground state atoms but the 2, 1, and 0 components bear little resemblance with the Ω PECs when properly calculated; see Fig. 1.

The lowest of the $^3\Pi$ states (see Fig. 4) correlating to the first Rydberg I atom features two potential minima of ion-pair and Rydberg character as was also the case in the E state of I_2.[47(a)] The global MRCI+SO+Q minimum of ion-pair character of the $\Omega = 2$ (r_e = 3.366 Å, ω_e = 174.7 cm^{-1}, $\omega_e x_e$ = 0.449 cm^{-1}, D_e = 100 kcal/mol, T_e = 39 446 cm^{-1}),

$\Omega = 1$ (r_e = 3.360 Å, ω_e = 174.5 cm^{-1}, $\omega_e x_e$ = 0.341 cm^{-1}, D_e = 99.3 kcal/mol, T_e = 42 007 cm^{-1}), and $\Omega = 0$ (r_e = 3.354 Å, ω_e = 175.5 cm^{-1}, $\omega_e x_e$ = 0.423 cm^{-1}, D_e = 92.0 kcal/mol, T_e = 44 570 cm^{-1}) PECs should be identified with the experimental D' 2 $(^3P_2)$ (r_e = 3.3502 Å, ω_e = 173.63 cm^{-1}, $\omega_e x_e$ = 0.5572 cm^{-1}, D_e = 96.2 kcal/mol, T_e = 39 061.83 cm^{-1}),[44,60] β 1 $(^3P_2)$ (r_e = 3.2930 Å, ω_e = 170.31 cm^{-1}, $\omega_e x_e$ = 0.4706 cm^{-1}, D_e = 96.1 kcal/mol, T_e = 39 103.67 cm^{-1}),[44,60] and E 0^+ $(^3P_2)$ (r_e = 3.2553 Å, ω_e = 165.69 cm^{-1}, $\omega_e x_e$ = 0.288 cm^{-1}, D_e = 96.2 kcal/mol, T_e = 39 059.48 cm^{-1}),[44,60] states, respectively, in very good agreement with the theoretical values. We should mention at this point that the experimental D_e values are given with respect to $I^+(^3P_2) + Cl^-(^1S_0)$ while the theoretical ones are calculated with respect to their adiabatic limits. The I atomic excitation energies calculated at the MRCI(+Q) level of theory of the supermolecule are in pleasant agreement with the experimental ones, i.e., $\Delta E(^4P \leftarrow \,^2P)$ = 6.734 (6.923) eV *vs* 6.886 (exp)[52] eV and $\Delta E(^2P \leftarrow \,^2P)$ = 7.007 (7.198) eV *vs* 6.934 (exp)[52] eV. The local minima of the $^3\Pi_{2,1,0}$ states are of purely Rydberg character, the outer electron is orbiting in a Rydberg σ $(6s6p_z)$ orbital. It is interesting to notice (see Fig. 4) that the local minima of all three SO components ($\Omega = 2, 1, 0$) suffer avoided crossings around their equilibrium distances with the repulsive parts of the same Ω symmetry PECs converging to the (2nd) $^3\Pi$ state dissociating to two ground ^2P atoms. The diabatic states though that can be formed from the two adiabatic ones have the following molecular MRCI+SO+Q constants $\Omega = 2$ (r_e = 2.234 Å, ω_e = 443.9 cm^{-1}, $\omega_e x_e$ = 0.837 cm^{-1}, T_e = 54 998 cm^{-1}), $\Omega = 1$ (r_e = 2.229 Å, ω_e = 446.3 cm^{-1}, $\omega_e x_e$ = 1.756 cm^{-1}, T_e = 57 196 cm^{-1}), and $\Omega = 0$ (r_e = 2.227 Å, ω_e = 447.4 cm^{-1}, $\omega_e x_e$ = 1.704 cm^{-1}, T_e = 59 330 cm^{-1}). Three more states ($\Omega = 2, 1, 0$) conclude the Rydberg states presently studied, $\Omega = 2$ (r_e = 2.278 Å, ω_e = 425 cm^{-1}, T_e = 62 535 cm^{-1}), $\Omega = 1$ (r_e = 2.278 Å, ω_e = 371 cm^{-1}, T_e = 64 630 cm^{-1}), and $\Omega = 0$ (r_e = 2.277 Å, ω_e = 387 cm^{-1}, T_e = 66 663 cm^{-1}). In Fig. 5 of Ref. 31 the PECs of all observed Rydberg states are sketched. We are therefore tempted to make the following correspondence $[^2\Pi_{3/2}]_c$ $6s^1\sigma$; $a_6(2)$ (T_e = 53 500 cm^{-1})[31,33] $\leftrightarrow$ $\Omega = 2$ (T_e = 54 998 cm^{-1}, local minimum of D'), $[^2\Pi_{1/2}]_c$ $6s^1\sigma$; $b_6(1)$ (T_e = 58 197 cm^{-1})[31] $\leftrightarrow$ $\Omega = 1$ (T_e = 57 196 cm^{-1}, local minimum of β), and $[^2\Pi_{1/2}]_c$ $6s^1\sigma$; $b_6'(0^+)$ (T_e = 57 557 cm^{-1})[31] $\leftrightarrow$ $\Omega = 0$ (T_e = 59 330 cm^{-1}, local minimum of E).

The last studied state in this work is the $^1\Pi_1$ correlating adiabatically to $I(5s^25p^46s^1, \,^2P) + Cl(^2P)$ but diabatically to the ion-pair $I^+(5s^25p^4, \,^1D) + Cl^-(^1S)$ through the intermediate of $I(5s^25p^46s^1, \,^2D) + Cl(^2P)$; see Fig. 3. Its PEC features two minima of ion-pair (r_e = 3.283 Å, ω_e = 184.1 cm^{-1}, $\omega_e x_e$ = 0.502 cm^{-1}, D_e = 81.6 kcal/mol, T_e = 48 171 cm^{-1}) and Rydberg character (r_e = 2.234 Å, ω_e = 455.8 cm^{-1}, $\omega_e x_e$ = 2.129 cm^{-1}, T_e = 56 203 cm^{-1}), practically identical to the $^3\Pi_0$ Rydberg minimum (*vide supra*). A second Rydberg minimum due to the $I(^2D)$ state is located at T_e = 76 558 cm^{-1} with r_e = 2.565 Å, ω_e = 260.9 cm^{-1}, $\omega_e x_e$ = 1.869 cm^{-1}. The ion-pair minimum should be identified with the H' 1 $(^1D_2)$ (ω_e = 184.03 cm^{-1}, T_e = 51 615 cm^{-1}) state observed for the first time in 1993.[34]

IV. CONCLUSIONS

We have constructed MRCI+SO potential energy curves for thirty nine Ω states of the diatomic ICl covering an energy range of $\sim 95\,000$ cm^{-1} employing effective core potentials and large Gaussian basis sets. The studied states converge adiabatically not only to ground state atoms but also to Rydberg dissociation channels. A general feature of the potential curves is the existence of numerous avoided crossings due to electrostatic and/or spin orbit effects creating an exciting vista for the appearance of non-adiabatic effects.[38] This is especially true for those curves that dissociate to Rydberg I atomic states and present potential minima of both Rydberg and ion-pair character. The extracted MRCI+SO molecular parameters are in acceptable agreement with the experimental data. However, by considering the +Q correction, the MRCI+SO+Q results are dramatically improved providing very good, and in some cases, excellent agreement with experiment. Thus the present study will serve preciously to the experimental community for the wealth of information it contains. The (inter)halogen diatomics proved to be of intrinsic difficulties due not only to the large number of electrons involved but also of the nature of the intervening excited states and we do hope that future theoretical work will focus on the specific problems raised herein.

[1] G. E. Gibson and H. C. Ramsperger, Phys. Rev. **30**, 598 (1927).
[2] G. E. Gibson and O. K. Rice, Nature (London) **123**, 347 (1929).
[3] E. Herbst and W. Steinmetz, J. Chem. Phys. **56**, 5342 (1972).
[4] F. E. Cummings and W. Klemperer, J. Chem. Phys. **60**, 2035 (1974).
[5] (a) R. D. Gordon and K. K. Innes, J. Chem. Phys. **71**, 2824 (1979); (b) R. D. Gordon and K. K. Innes, J. Mol. Spectrosc. **78**, 350 (1979).
[6] M. S. de Vries, N. J. A. van Veen, M. Hutchinson, and A. E. de Vries, Chem. Phys. **51**, 159 (1980).
[7] R. E. Willis, Jr. and W. W. Clark III, J. Chem. Phys. **72**, 4946 (1980).
[8] J. A. Coxon, R. M. Gordon, and M. A. Wickramammratchi, J. Mol. Spectrosc. **79**, 363 (1980).
[9] J. A. Coxon and M. A. Wickramammratchi, J. Mol. Spectrosc. **79**, 380 (1980).
[10] J. C. D. Brand, D. Bussières, A. R. Hoy, and S. M. Jaywant, Can. J. Phys. **62**, 1947 (1984); Chem. Phys. Lett. **109**, 101 (1984).
[11] J. D. Spivey, J. G. Ashmore, and J. Tellinghuisen, Chem. Phys. Lett. **109**, 456 (1984).
[12] T. Suzuki and T. Kasuya, J. Chem. Phys. **81**, 4818 (1984).
[13] J. C. D. Brand, D. Bussières, and A. R. Hoy, Mol. Phys. **53**, 525 (1984).
[14] M. Siese, F. Bässmann, and E. Tiemann, Chem. Phys. **99**, 467 (1985).
[15] J. C. D. Brand, D. Bussières, and A. R. Hoy, J. Mol. Spectrosc. **113**, 388 (1985).
[16] J. C. D. Brand and A. R. Hoy, J. Mol. Spectrosc. **114**, 197, 219 (1985).
[17] J. B. Hudson, L. J. Sauls, P. C. Tellinghuisen, and J. Tellinghuisen, J. Mol. Spectrosc. **148**, 50 (1991).
[18] A. Pardo, J. J. Camacho, and J. M. L. Payato, J. Chem. Soc. Faraday Trans. **87**, 2529 (1991).
[19] H. G. Hedderich, P. F. Bernath, and G. A. McRae, J. Mol. Spectrosc. **155**, 384 (1992).
[20] A. Durand, J. C. Loison, and J. Vigué, J. Chem. Phys. **101**, 3514 (1994); **106**, 477 (1997).
[21] S. X. Wang, J. L. Booth, F. W. Dalby, and I. Ozier, J. Chem. Phys. **101**, 5464 (1994).
[22] T. J. Slotterback, S. G. Clement, K. C. Janda, and C. M. Western, J. Chem. Phys. **101**, 7221 (1994).
[23] T. A. Takei, A. Watanabe, and Y. Amako, J. Mol. Spectrosc. **171**, 287 (1995); J. Chem. Phys. **110**, 10874 (1999).
[24] W. S. Barney, C. M. Western, and K. C. Janda, J. Chem. Phys. **113**, 7211 (2000).
[25] R. H. Barnes, C. E. Moeller, J. F. Kircher, and C. M. Verber, Appl. Phys. Lett. **24**, 610 (1974).
[26] G. W. King, I. M. Littlewood, R. G. McFadden, and J. R. Robins, Chem. Phys. **41**, 379 (1979).
[27] J. C. D. Brand, U. D. Deshpande, A. R. Hoy, and S. M. Jaywant, J. Mol. Spectrosc. **100**, 416 (1983).
[28] D. Bussières and A. R. Hoy, Can. J. Phys. **62**, 1941 (1984).
[29] J. C. D. Brand, A. R. Hoy, and S. M. Jaywant, J. Mol. Spectrosc. **106**, 388 (1984).
[30] R. H. Lipson and A. R. Hoy, J. Chem. Phys. **90**, 6821 (1989).
[31] K. P. Lawley, E. A. Kerr, R. J. Donovan, A. Hopkirk, D. Shaw, and A. J. Yencha, J. Phys. Chem. **94**, 6201 (1990).
[32] M. A. Stepp, M. A. Kremer, P. C. Tellinghuisen, and J. Tellinghuisen, J. Mol. Spectrosc. **146**, 169 (1991).
[33] R. J. Donovan, T. Ridley, K. P. Lawley, and P. J. Wilson, Chem. Phys. Lett. **205**, 129 (1993).
[34] R. J. Donovan, K. P. Lawley, T. Ridley and P. J. Wilson, Chem. Phys. Lett. **207**, 129 (1993).
[35] R. J. Donovan, J. G. Goode, K. P. Lawley, T. Ridley, and A. J. Yencha, J. Phys. Chem. **98**, 2236 (1994).
[36] T. Ridley, D. A. Beattie, M. C. R. Cockett, K. P. Lawley, and R. J. Donovan, Phys. Chem. Chem. Phys. **4**, 1398 (2002).
[37] K. P. Lawley, A. C. Flexen, R. R. J. Maier, A. Monck, T. Ridley, and R. J. Donovan, Phys. Chem. Chem. Phys. **4**, 1412 (2002).
[38] H. Lefebvre-Brion and R. W. Field, *The Spectra and Dynamics of Diatomic Molecules* (Elsevier, Amsterdam, 2004).
[39] K. Balasubramanian, J. Mol. Spectrosc. **110**, 339 (1985); Chem. Phys. **95**, 225 (1985).
[40] N. Diamantopoulou, A. Katrakoulis, P. Glodic, T. N. Kitsopoulos, and P. C. Samartzis, J. Chem. Phys. **134**, 194314 (2011).
[41] P. C. Samartzis and T. N. Kitsopoulos, J. Chem. Phys. **133**, 014301 (2010).
[42] (a) K. Tonokura, Y. Matsumi, M. Kawasaki, H. L. Kim, S. Yabushita, S. Fujimura, and K. Saito, J. Chem. Phys. **99**, 3461 (1993); (b) S. Yabushita, J. Mol. Struct.: THEOCHEM **461–462**, 523 (1999); (c) T. Matsuoka, S. Oonishi, and S. Yabushita, Int. J. Quantum Chem. **113**, 375 (2013); (d) T. Matsuoka and S. Yabushita, Chem. Phys. Lett. **592**, 75 (2014).
[43] A. J. Alexander and T. P. Rakitzis, Mol. Phys. **103**, 1665 (2005).
[44] V. A. Alekseyev, Opt. Spectrosc. **99**, 719 (2005).
[45] A. J. Sadlej, J. Chem. Phys. **96**, 2048 (1992); S. A. Perera and R. J. Bartlett, Chem. Phys. Lett. **216**, 606 (1993); W. A. de Jong, J. Styszynski, L. Visscher, and W. C. Nieuwpoort, J. Chem. Phys. **108**, 5177 (1998); A. Zaitsevskii, C. Teichteil, J. Vigué, and G. Bazalgette, Chem. Phys. Lett. **307**, 277 (1999).
[46] A. S. Bogomolov, B. Grüner, S. A. Kochubei, M. Mudrich, and A. V. Baklanov, J. Chem. Phys. **140**, 124311 (2014).
[47] (a) A. Kalemos, A. Valdés, and R. Prosmiti, J. Phys. Chem. A **116**, 2366 (2012); **117**, 790 (2013); (b) A. A. Vassilakis, A. Kalemos, and A. Mavridis, Theor. Chem. Acc. **133**, 1436 (2014).
[48] J. P. Darr and R. A. Loomis, J. Chem. Phys. **129**, 144306 (2008).
[49] A. Valdés, R. Prosmiti, P. Villarreal, and G. Delgado-Barrio, J. Chem. Phys. **135**, 244309 (2011); **125**, 014313 (2006); R. Prosmiti, C. Cunha, G. Delgado-Barrio, and P. Villarreal, J. Chem. Phys. **117**, 7017 (2002).
[50] M. P. De Lara-Castells, R. Prosmiti, G. Delgado-Barrio, D. López-Durán, P. Villarreal, F. A. Gianturco, and J. Jellinek, Phys. Rev. A **74**, 054611 (2006); A. Valdés, and R. Prosmiti, J. Phys. Chem. A **117**, 7217 (2013).
[51] P. Glodic, A. Kartakoullis, M. Fárník, P. C. Samartzis, and T. N. Kitsopoulos, J. Chem. Phys. **137**, 154306 (2012).
[52] (a) C. E. Moore, NSRDS–NBS 35 (1971); (b) A. Kramida, Yu. Ralchenko, J. Reader, and NIST ASD Team, NIST Atomic Spectra Database, version 5.1, National Institute of Standards and Technology, Gaithersburg, MD, 2013, see http://physics.nist.gov/asd.
[53] (a) H.-J. Werner and P. J. Knowles, J. Chem. Phys. **89**, 5803 (1988); P. J. Knowles and H.-J. Werner, Chem. Phys. Lett. **145**, 514 (1988);

K. R. Shamasundar, G. Knizia, and H.-J. Werner, J. Chem. Phys. **135**, 054101 (2011); P. J. Knowles and H.-J. Werner, Theor. Chim. Acta **84**, 95 (1992); (b) P. J. Knowles, C. Hampel, and H.-J. Werner, J. Chem. Phys. **99**, 5219 (1993); **112**, 3106 (2000) (Erratum); (c) H.-J. Werner and P. J. Knowles, *ibid.* **82**, 5053 (1985); P. J. Knowles and H.-J. Werner, Chem. Phys. Lett. **115**, 259 (1985); (d) A. Berning, M. Schweizer, H.-J. Werner, P. J. Knowles, and P. Palmieri, Mol. Phys. **98**, 1823 (2000).

[54](a) K. A. Peterson, B. C. Shepler, D. Figgen, and H. Stoll, J. Phys. Chem. A **110**, 13877 (2006); (b) T. H. Dunning, Jr., K. A. Peterson, and A. K. Wilson, J. Chem. Phys. **114**, 9244 (2001); (c) K. A. Peterson and K. E. Yousaf, *ibid.* **133**, 174116 (2010); (d) K. A. Peterson and T. H. Dunning, Jr., *ibid.* **117**, 10548 (2002).

[55]J. L. Dunham, Phys. Rev. **41**, 721 (1932).

[56]H.-J. Werner, P. J. Knowles, G. Knizia, F. R. Manby, M. Schütz *et al.*, MOLPRO, version 2012.1, a package of *ab initio* programs, 2012, see http://www.molpro.net.

[57]C. F. Bunge, J. A. Barrientos, and A. V. Bunge, At. Data Nucl. Data Tables **53**, 113 (1993).

[58]It was incorrectly believed that this state dissociates adiabatically to $I(^2P_{3/2})$ + $Cl(^2P_{3/2})$, see Ref. 15.

[59]T. P. Rakitzis, S. A. Kandel, A. J. Alexander, Z. H. Kim, R. N. Zare, Science **281**, 1346 (1998); T. P. Rakitzis, S. A. Kandel, A. J. Alexander, Z. H. Kim, R. N. Zare, J. Chem. Phys. **110**, 3351 (1999).

[60]J. C. D. Brand and A. R. Hoy, Appl. Spectrosc. Rev. **23**, 285 (1987).